ARCHIVES OF ELECTRICAL ENGINEERING VOL. 61(4), pp. 597-608 (2012)

DOI 10.2478/v10171-012-0044-9

Energy absorption by ferromagnetic nanoparticles in hyperthermia therapy

EUGENIUSZ KURGAN

Department of Electrical and Power Engineering
AGH University of Science and Technology
al. Mickiewicza 30, 30-059 Kraków, Poland
e-mail: kurgan@agh.edu.pl

(Received: 04.04.2012, revised: 27.06.2012)

Abstract: A numerical method is developed for estimation of temperature distributions inside tissues heated by external RF hyperthermia with external circular coil. The computational method relies on a solution of electromagnetic field problem in sinusoidal steady state. The heat transfer problem is treated in three dimensions with axis symmetry model. Than the bioheat diffusion equation under a steady-state condition is solved to determine the temperature distributions inside tumour and surrounding tissues. The heat removal due to the blood circulation is also taken into account. Numerical results are presented for heat generated by ferromagnetic nanoparticles in order to minimize negative effects of radiofrequency radiation.

Key words: evolutionary algorithm, parametric optimization, DC electric series motor

1. Introduction

Thermal transport, electromagnetic field distribution within living organisms, bioheat transfer and other aspects of electromagnetic-heat relations, are an important biological and therapeutic issue, which includes new aspects in thermal therapies, cryobiology, burn injury and disease diagnostics. Thermal side effects of various treatments are important issues in bioheat investigations such as in hyperthermia. A principal issue in medical thermal therapeutic applications, such as hyperthermia treatment, is modelling and understanding the heat transport and temperature distribution within biological tissues and different body structures [1].

Hyperthermia therapy is accepted as the fourth additional cancer treatment technique following surgery, chemotherapy, and radiation techniques. In hyperthermia, the tumour cells are overheated to a therapeutic value, typically 40-45°C to damage the cancer cells and to avoid the effect of metastases. Although it is known for many years that fever can damage the tumour cells, hyperthermia technique in last decades is being developed as a cancer treatment by generating and concentrating the heat on the cancer cells. Hyperthermia is being used for

many cancer types such as melanomas, breast cancer, bone metastases, carcinomas of the lung, stomach, pancreas, gallbladder, kidneys, neck, brain tumours, prostate tumours, and cervical cancer [2].

In distinction to healthy cells, a tumour is a tightly placed body of cells in which the blood circulation is limited. Heat can reduce the oxygen and nutrients from the abnormal cells causing a failure in the tumour's vascular system and damage of the cell's metabolism and consequent devastation of tumour cells. Additionally, heat causes the creation of certain proteins in the unhealthy cancer cells, the so-called heat shock proteins, which are formed on the surface of the degenerated cells. The body immune system treats these proteins as foreign cells, making the abnormal that is the tumour cells visible to the immune system [3].

Hyperthermia technique also improves the efficiency of other cancer therapies such as, chemotherapy and radiotherapy. These cells, which not respond to chemotherapy or radiation, should be subjected to heat treatment. Hyperthermia in combination with chemotherapy causes the drug to penetrate deeper into the tumour cells while amplifying the efficiency of the drug delivered to the tumour. The increased efficacy of simultaneous use of hyperthermia and radiotherapy or chemotherapy has been demonstrated in treatment of certain types of diseases [3], such as breast cancer [6], cervical and bladder cancer [2], rectal cancer [4], prostate cancer [5], head and neck cancer [6] and lung and stomach cancer.

Hyperthermia therapy can be applied either on the whole body or locally targeting the tumour cells. Whole body hyperthermia treatment is usually applied for metastases, which have disseminated throughout the body, and for frequently recurring tumour types. Localized hyperthermia therapy can be achieved in this way so it can guarantee a relatively reduced effect on healthy cells while a higher temperature is attained in the cancer cells. One of the important problems in hyperthermia is to apply the treatment mainly on the abnormal cells to avoid burning and destroying the healthy ones. Near surface hyperthermia is achieved using various methods such as warm water bath balloons and blankets, hot wax, coils with exciting currents and thermal chambers. For deep localized hyperthermia various physical phenomenon's such as short waves, ultra-high frequency sound waves, microwave and laser can be utilized [7].

2. Magnetic nanoparticles

Magnetic targeting of cancerous tissue employing multifunctional carrier nanoparticles has the possibility to provide more effective anticancer therapy by permitting a diversity of localized treatment and diagnostic methods, while at the same time decreasing undesired side effects. Interest in this therapy is growing because the recent improvement in the development of carrier particles that are created to target a particular tissue, and influence local chemo-, radio- and genetherapy at a tumour site.

Magnetic carrier particles consist of a nonmagnetic core material, such as polyacrylamide [9], with embedded magnetic nanoparticles and therapeutic agents such as photodynamic sensitizers (Fig. 1). Polyethylene glycol and biotargeting agents can be coated onto the surface

of the carrier particle to control plasma residence time and to promote binding to target tissue, respectively [9]. The magnetic nanoparticles inserted in the carrier particle permit multiple, distinct therapeutic functions including magnetic therapy, RF hyperthermia and magnetic resonance imaging (MRI) contrast enhancement.

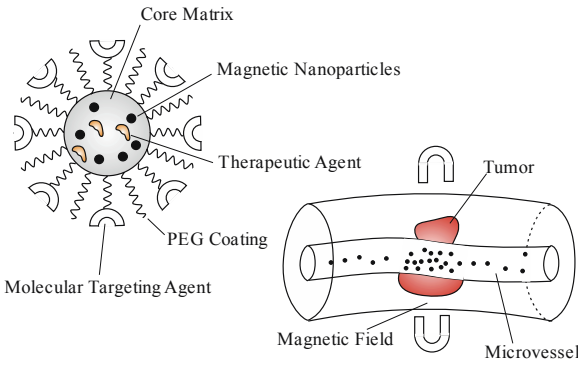

Fig. 1. Magnetic targeting by multifunctional carrier particles [8]

A potential advantage of using magnetic nanoparticles is the use of localized magnetic field gradients to attract the particles to a chosen places, and to hold them there until the therapy is complete and then in this or other way to remove them from organism. This creates a problem of design an arrangements, which are capable to generate enough strong magnetic field and simultaneously be easy to maintain. The desired portion of particles may be injected in water solution intravenously, and then blood pressure would be used to transport the particles to the site of interest for treatment. Alternatively in many cases the particles suspension could be introduce directly into the treatment area. Either of these methods has the requirement that the particles do not aggregate and block their own movement in blood. By MRI technics position of this particles can be control with enough precision [8].

Magnetic nanoparticles used in medical applications have sizes ranging from a few nanometers up to thousands of nanometers, what means that their dimensions are smaller than or comparable to those of a cell (10-100 μm), a protein (5-50 nm), a virus (20-450 nm), or a gene (2 nm wide and 10-100 nm long). Because of this they can to come in direct vicinity of biological tissues of interest. Such nanoparticles should be coated with biological molecules, such as a starch, to make them difficult to recognize by an organism's immune defence system, thereby providing a possibility to control the means of transport them to desire places. The nanoparticles are magnetic, what means that they obey Lorenz's low, what gives possibility to manipulate them by an external magnetic field with high magnetic gradient. This property of magnetic nanoparticles enables location of them in desired places. Next, magnetic nanoparticles can be made to respond to time varying electromagnetic field, what results in transfer of energy from external exciting energy sources to nanoparticles and in this way to treated tissues.

Several authors have considered the heat generation problem here given volume of tumour was heated by evenly placed heat sources such as magnetic nanoparticles or seeds. However,

it is often-assumed that a heat generation in amount of 100 mW/cm^3 will suffice in most circumstances to heat a tissue. The generating heat is limited by many harmful physiological reactions of the healthy tissues to high frequency and strength the externally applied AC magnetic field used in hyperthermia. The negative effects incorporate stimulation of peripheral and skeletal muscles, eventual cardiac stimulation and arrhythmia and eddy-current e heating of tissues. It is assumed, that the useful range of frequencies and magnetic strength is considered to be in the range f = 50-1200 kHz and H = 0-15 kAm^{-1}. Another authors report that exposure to field should fulfil a condition that product of magnetic strength and frequency $H{\cdot}f$ should not exceed $4.85 \times 108 = 523.8$ Am^{-1}s^{-1} in order to be tolerable. The methods of administration of the nanoparticles suspended in liquid decide about the amount of magnetic material required to produce the desired temperature. So, the direct injection of the therapeutic agent allows for significantly greater quantities of nanoparticles to be localized in a tumour than do methods utilizing intravascular administration or antibody targeting. One can assume that about 5-10 mg of magnetic nanoparticles should be comprised in each cm^3 of tumour tissue is suitable for magnetic hyperthermia.

3. Energy losses in nanoparticles

Losses occurring in nanomagnetic particles may be divided in three general types: relaxational losses, hysteresis losses, and resonance losses. Relaxational losses, which dominate in dimension range up to several hundred micrometers, are divided in two classes: Brown losses resulting from reorientation of the magnetic particle itself in the fluid and Néel losses resulting from reorientation of the magnetic moment in a particle. In the first instance viscous friction and in the second case anisotropy barrier determines relaxation time. Hysteresis losses dominate for particles in the range micrometers. They are proportional to the hysteresis loop surface and frequency of the exciting magnetic field. Resonance losses can also in some circumstances give significant participation in total losses.

The rise of magnetization M produced by the increase of field intensity H progresses in three main stages-initial reversible magnetization, rapid irreversible magnetization and the slow approach to saturation, related respectively to the reversible shifts of domain walls, irreversible rotation and shifts processes and the reversible rotation of domains [9]. The typical dependence of the magnetic induction from magnetic field is given by

$$B = \mu_0 (M + H). \tag{1}$$

The initial part of this relation satisfies the Rayleigh formula

$$B = \mu_0 (M + H), \tag{2}$$

where the first term symbolizes the reversible component, and the quadratic term the irreversible component of magnetization. The more suitable description of the magnetization curve is more complicated. Completely reversible anhysteretic magnetization curve may be described by the theoretical Brillouin Equation [9]

$$\frac{M(H)}{M_s} = \frac{2J+1}{2J}\coth\left(\frac{2J+1}{2J}\frac{H}{a}\right) - \frac{1}{2J}\coth\left(\frac{1}{2J}\frac{H}{a}\right), \tag{3}$$

where M_s is the saturation magnetization, J is quantum number and a is shape parameter dependent on material properties. The above relation can be approximated the two extreme estimates of this Equation [9]

- approximation with a moment of one spin per atom (J = ½), which reduces the above equation to the tangent hyperbolic function

$$\frac{M(H)}{M_s} = \tanh\left(\frac{H}{a}\right), \tag{4}$$

- classical approximation, where $J \to \infty$ and in this case (3) becomes Langevin function

$$\frac{M(H)}{M_s} = \coth\left(\frac{H}{a}\right) - \frac{a}{H} = L\left(\frac{H}{a}\right), \tag{5}$$

The accuracy of these approximations in a wider region of magnetization is not high, and the first two models require numerical calculations [10]. Thus we will attempt to find an approximation based on the Brillouin equation satisfying the following conditions

- it should be consistent with the phenomenological description of magnetization,
- its parameters have clear physical meaning,
- it achieves high accuracy in the whole region of magnetization.

Following approximation should satisfy the above conditions

$$M(H) = M_a L\left(\frac{H}{a}\right) + M_b \tanh\left(\frac{|H|}{b}\right) L\left(\frac{H}{b}\right), \tag{6}$$

where M_a, M_b express the reversible and irreversible components of saturation magnetization, and a, b determine the rate of their approach to saturation. This equation can be used for the approximation of typical magnetization curve. If saturation magnetization $M_s = M_a + M_b$ is known from the catalogues, it has only three adjustable parameters.

In reality the magnetization does not change along the commutation curve, but along two branches of hysteresis loops $B_\pm$ situated above and below this curve. Typical smaller loops of amplitude H_m are described by the second Rayleigh relation [9]

$$B_\pm = \mu_0\left[M_a L\left(\frac{H}{a}\right) + M_b \tanh\left(\frac{H_m}{b}\right)\cdot L\left(\frac{H \pm c\tanh(H_m/2c)(1-(H^2/H_m^2))}{b}\right) + H\right], \tag{7}$$

where c denotes the field at which the irreversible component of magnetization along a major hysteresis loop is equal to zero. With the assumption of the uniform distribution of the sinusoidal magnetic field in nanoparticles, the eddy current losses in the unit volume of a core per one cycle of magnetization are given by the formula [9]

$$W_e = \frac{2f(\pi R B_m)^2}{3}\sigma, \tag{8}$$

where f is the frequency, R the radius of the nanoparticle, σ the conductivity of particle and B_m the amplitude of magnetic induction in given place. This relation can be directly used to determine the heat generated by ferromagnetic nanoparticles.

4. Field equations

Around the human body, at a some distance, circular coil with excitation current is placed. The human body is considered as homogeneous medium with averaging material parameters. It is assumed that human body has an ellipsoidal shape with semiexes a and b. Tumour inside the body has a circular form with radius r. Moreover radius of the outer dimension of the wire has value r_2 and the radius of the inner dimension has the value r_1. The exciting current in the wires generates sinusoidal electromagnetic field which next induces eddy currents in human body. These currents are sources of heat and after some transient time a temperature distribution in body are established. In order to calculate temperature distribution electromagnetic field distribution generated by wires with exciting currents has to be calculated.

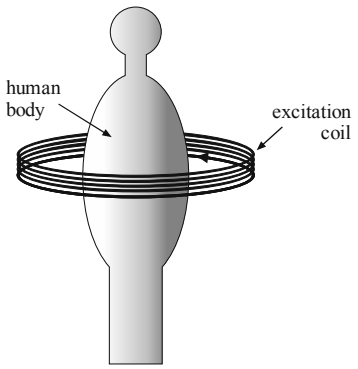

Fig. 2. Schematic view of human body surrounded by wire with excitation current

In this article it is assumed that heat generation is only caused by hysteresis losses. The hysteresis loss is a consequence of the nonlinear properties of magnetic materials exposed to a time varying magnetic field and is proportional to the area of the hysteresis loop and frequency of the exiting source.

Let us start with equation for magnetic potential in frequency domain. The vector potential $\mathbf{A} = \mathbf{A}(x, y)$ is parallel to $x - y$ plane. Equation for magnetic potential is given by

$$\nabla \times \left(\frac{1}{\mu} \times \hat{\mathbf{A}} \right) + \left(j\omega\sigma - \omega^2 \varepsilon \right) \hat{\mathbf{A}} = \hat{\mathbf{J}}_{\mathrm{i}}, \tag{9}$$

where $\hat{\mathbf{A}}$ is magnetic vector potential, $\hat{\mathbf{J}}_{\mathrm{i}}$ is external impressed current density, μ is magnetic permeability, σ is electric conductivity, ε is electric permittivity and ω is angular frequency.

The electrical properties of tissues and cell suspensions could be expressed by frequency dependence over the whole frequency range from a few Hz to many GHz.

$$\hat{\varepsilon}(\omega) = \varepsilon_\infty + \sum_{n=1}^{4} \frac{\Delta\varepsilon_n}{1 + (j\omega\tau_n)^{1-\alpha_n}} - j\frac{\sigma}{\omega\varepsilon_0}. \tag{10}$$

This equation is subsequently used to determine dielectric properties of all tissues. Necessary constant coefficients are taken from [4] and are not reproduced here

$$\hat{\varepsilon}(\omega) = \varepsilon' + j\varepsilon''. \tag{11}$$

Because in this case potential has following two components

$$\hat{\mathbf{A}} = \hat{A}_x \mathbf{a}_x + \hat{A}_y \mathbf{a}_y \tag{12}$$

and external current density has the same form

$$\hat{\mathbf{J}}_i = \hat{J}_x \mathbf{a}_x + \hat{J}_y \mathbf{a}_y. \tag{13}$$

Taken the above considerations into account, in end effect we obtained two equations in complex variables for both parts of vector potential:

$$\nabla \cdot \left(\frac{1}{\mu} \nabla \hat{A}_x \right) + \left(\omega^2 \varepsilon' + j\omega(\omega\varepsilon'' - \sigma) \right) \hat{A}_x = -\hat{J}_x, \tag{14}$$

$$\nabla \cdot \left(\frac{1}{\mu} \nabla \hat{A}_y \right) + \left(\omega^2 \varepsilon' + j\omega(\omega\varepsilon'' - \sigma) \right) \hat{A}_y = -\hat{J}_y. \tag{15}$$

5. Heat equation

Unlike the computation of the electric currents in body, for which agreement exists accordingly a derived physical model, no clear consensus exists for an appropriate mathematical model for the evaluation of temperature field distribution in biological tissues. An extremely important work in the modelling of heat transfer in biological tissues was done over half a century ago by Pennes. The equation, which he derived, is named bioheat equation, and it can be derived from the classical Fourier law of heat conduction.

This model is based on the simple assumption of the energy exchange between the blood flowing in vessels and the surrounding the tumour tissues. Pennes model may provide suitable information on temperature distributions in whole body, organ under consideration, and tumour analysis under study. Pennes model states, that the total heat ex-change between tissue surrounding a vessel and blood flowing in it, is proportional to the volumetric heat flow and the temperature difference between the blood and the tissue. The expression of Pennes bioheat equation in a body with uniform material proper-ties in steady state is given by

Heat transport through the biological tissues, represented by bioheat models, involves thermal conduction in tissue and vascular system, blood–tissue convection and perfusion (through capillary tubes within the tissues) and also metabolic heat Analytical and computational studies have been done utilizing stated bioheat transfer models and the local thermal equilibrium assumption between the blood and the tissue. Some bioheat models are also established and examined for counter current heat transfer in arterial-venous vessels

$$\nabla(-k\nabla T) = \rho_b C_b \omega_b (T_b - T) + Q_{eddy} + Q_{met} + W_s \,, \tag{16}$$

where T is body temperature [K], k − the tissue thermal conductivity [W/(m K)], ω_b − the blood perfusion rate [1/s], C_b − the blood specific heat, T_b − the blood vessel temperature, Q_{met} − the metabolic heat generation rate [W/m^3], Q_{ext} − the external heat sources [W/m^3]m and W_s is the power generated by hysteresis losses [W/m^3]. The usual boundary condition associated with the heat transfer process in the context of hyperthermia can be given by $T = T_{\text{air}}$.

6. Numerical example

It was assumed that tumour occurs in liver as in Figure 1 right. The amount of 10 mg/cm^3 nanoparticles was injected into tumour and uniformly inside distributed. Geometrical dimension are given in Figure 1. Exciting wirers with current have parameters $I_{\max} = 1e^4$ [A], $r_5 =$ $= 0.01$ [m] and frequency $f = 100$ [MHz], Physical parameters of blood are as follows: $\rho_b =$ $= 1060$ [kg/m^3], $C_b = 3639$ [J/(kg·K)], $T_b = 310.15$ [K], $\omega_b = 0.005$ [1/s]. Physical parameters of tissues are given by: relative permittivity $\varepsilon_r = 29.6$ in body, 70 in tumour and 5.8 in liver, electric conductivity $\sigma = 0.02$[S/m] in tumour, body and skin and 0.002 [S/m] in liver. The hysteresis loss for one loop is $5{\cdot}10^{-4}$ J/g when $H_0 = 35$ kA/m. The frequency was assumed $f = 100$ kHz. The exciting current was so adjusted to attain specific loss power 400, 450 and 500 mW/cm^3.

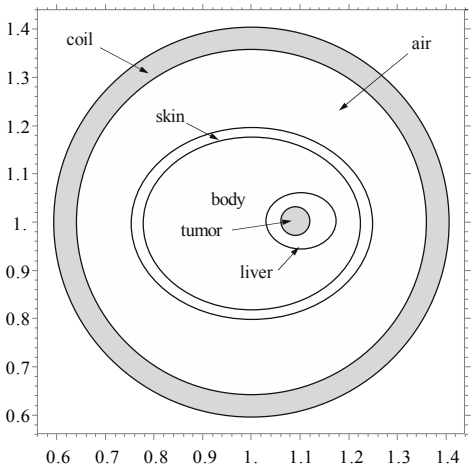

Fig. 3. Cross section through human body together with coil

All electrical properties of all tissues are taken from [10] and are not quoted here. Only dependence of both parts of complex permittivity for liver computed from equation are shown in Figure 3. One can see that relative permittivity for radio frequency range (up to 100 Mhz) assumes very large values. Only for gigahertz frequencies it has permittivities comparable with that for water.

After solution Equations (14) and (15) with finite element method magnetic potential in computational domain was obtained. In Figure 5 dependence of modulus of potential **A** along body cross section is presented. There are two sources of heat generation in human body. One is resulting from power generated by eddy current and the second, by hysteresis in ferromagnetic nanoparticles (Figs. 6, 7).

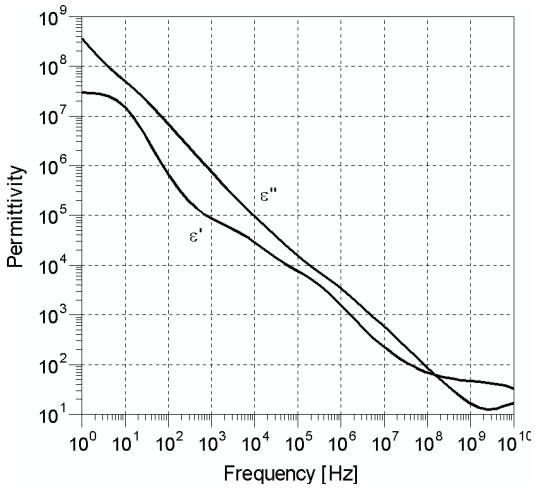

Fig. 4. Real and imaginary parts of the complex permittivity

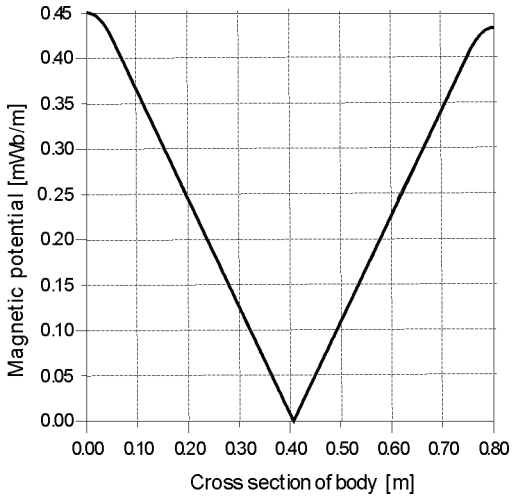

Fig. 5. Modulus of the magnetic vector potential **A** versus body cross section

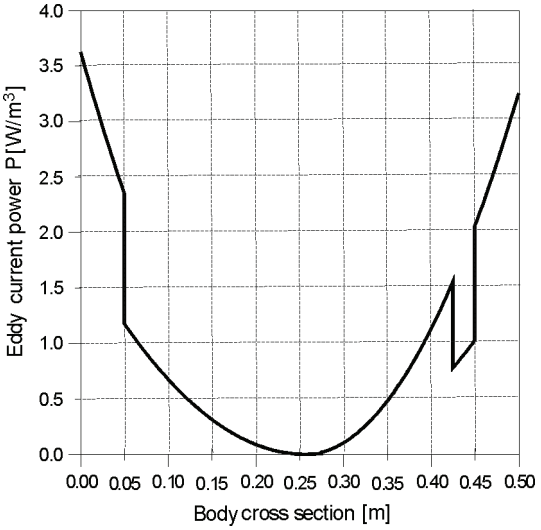

Fig. 6. Power dissipated by eddy current along body cross section

Power generated by eddy currents is distributed over whole body cross-section and heat generated by ferromagnetic nanoparticles is restricted only to tumour tissues. The power generated by ferromagnetic particles is in tumour more than 30 times greater than that generated by eddy currents and from practical point of view can be neglected.

Next bio-heat equation (16) is solved. The term $\rho_b C_b \omega_b (T_b - T)$ on the right hand side of this equation represents the heat carried away by blood in arteries and veins. In Figures 7 and 8 temperatures along tumour perimeter and along body cross section is shown. In both cases temperature in the tumour is above 42°C what guarantees destruction of tumour tissues.

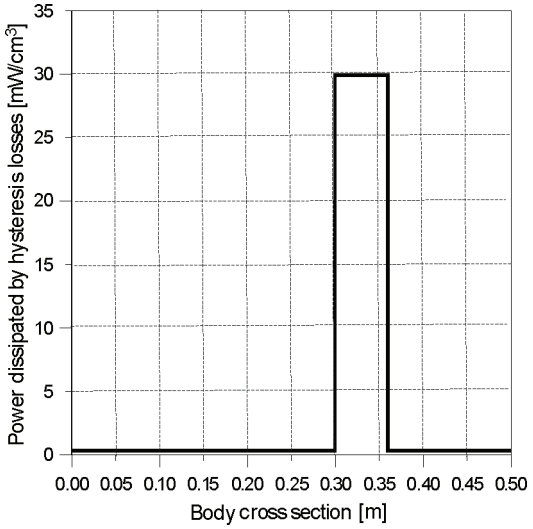

Fig. 7. Power dissipated in tumour by hysteresis losses

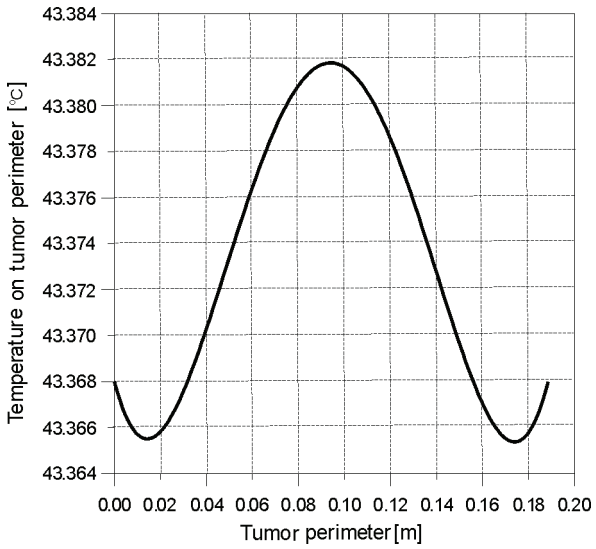

Fig. 8. Temperature distribution along tumour perimeter

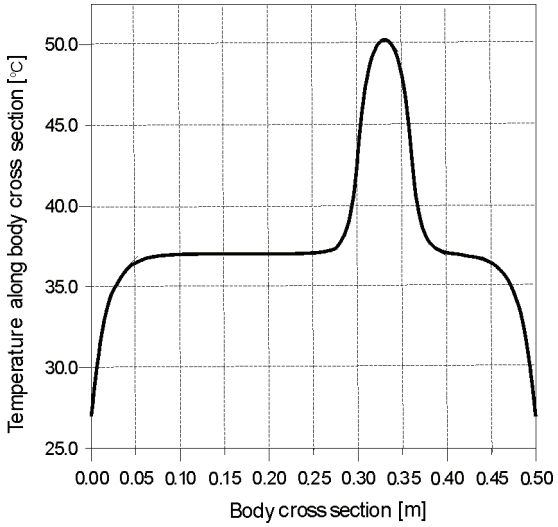

Fig. 9. Temperature distribution along body cross section

7. Conclusions

Theoretical studies of temperature distributions obtained with magnetic induction methods of achieving hyperthermia have been presented. By nanoparticle heating using hysteresis losses one can obtain temperature distribution in over 42 °C range. The developed procedure is general and could be used to evaluate temperature distributions for arbitrary coils configu-

rations, also in the case when coils are placed at different angels compared with human body, have different radius and different conducting currents. The described method could be used to optimize the position, exciting current amplitude and phases of coils, and to give better control to the temperature distributions throughout the tumour volume. Because most heat is generated in tumour, where ferromagnetic nanoparticles occur, the harmful effect of electromagnetic radiation can be minimalized.

References

[1] Hall E.J., Roizin-Towle L., *Biological effects of heat.* Cancer Res. 44: 4708s-4713s (1984).
[2] Field S.B., Hand J.W., *An Introduction to the Practical Aspects of Clinical Hyperthermia.* Taylor & Francis, New York (1990).
[3] Wust P., Hildebrandt B., Sreenivasa G. et al., *Hyperthermia in combined treatment of cancer.* Lancet Oncol. 3(8): 487-497 (2002).
[4] Zee J., Gonzalez D., Rhoon G. et al., *Comparison of radiotherapy alone with radiotherapy plus hyperthermia in locally advanced pelvic tumours: a prospective, randomised, multicentre trial.* Lancet 355(9210): 1119-1125 (2000).
[5] van Vulpen M., de Leeuw A.A.C., Raaymakers B.W. et al., *Radiotherapy and hyperthermia in the treatment of patients with locally advanced prostate cancer: preliminary results.* BJU Int. 93(1): 36-41 (2004).
[6] Vernon C.C., Hand J.W., Field S.B. et al., *Radiotherapy with or without hyperthermia in the treatment of superficial localized breast cancer: results from five randomized controlled trials.* Int. J. Radiat. Oncol. Biol. Phys. 35(4): 731-744 (1996).
[7] Charny C.K., *Mathematical models of bioheat transfer.* Adv. Heat Transfer 22: 19-155 (1992).
[8] Furlani E.J., Furlani E.P., *A model for predicting magnetic targeting of multifunctional particles in the microvasculature.* Journal of Magnetism and Magnetic Materials 312: 187-193 (2007).
[9] Włodarski Z., *Analytical description of magnetization curves*. Physica B, 373: 323-327 (2006).
[10] Gabriel C., Gabriel S., *Compilation of the dielectric properties of body tissues at RF and microwave frequencies.* Physics Department, King's College, London, WC2R 2LS, UK, June (1996).